Complex Microstructured 3D Surfaces Using Chitosan Biopolymer

Javier G. Fernandez, Christopher A. Mills, and Josep Samitier*

***A** technique for producing micrometer-scale structures over large, non-planar chitosan surfaces is described. The technique makes use of the rheological characteristics (deformability) of the chitosan to create free-standing, three-dimensional scaffolds with controlled shapes, incorporating defined microtopography. The results of an investigation into the technical limits of molding different combinations of shapes and microtopographies are presented, highlighting the versatility of the technique when used irrespectively with inorganic or delicate organic moulds. The final, replicated scaffolds presented here are patterned with arrays of one-micrometer-tall microstructures over large areas. Structural integrity is characterized by the measurement of structural degradation. Human umbilical vein endothelial cells cultured on a tubular scaffold show that early cell growth is conditioned by the microtopography and indicate possible uses for the structures in biomedical applications. For those applications requiring improved chemical and mechanical resistance, the structures can be replicated in poly(dimethyl siloxane).*

Keywords:
- biopolymers
- chitosan
- microstructures
- surfaces

1. Introduction

Topography at the microscale and nanoscale can determine the physico-chemical properties of a surface at the macroscale. Physical properties, including the coefficient of friction and surface energy (contact angle), and optical effects, such as gloss and color, can be tuned by control of the surface structure at (sub)micrometer levels. Applications for such surfaces, with accurately controlled surface topographies, are present in practically all engineering fields. For example, bioengineers have paid special attention to cells cultured on substrates that contain a defined topography at dimensions where cell interactions occur. Altering the surface topography allows these interactions to be controlled and, hence, the behavior of the cells.[1]

At present, several simple, low-cost tools exist, which are applicable to bioengineering, for the fabrication of micro- and nanostructures on biocompatible surfaces.[2] Such structures have defined form, dimensions, and separation, giving rise to controlled surface characteristics, which consequently can be used to adapt cell growth and functionality.[3] However, all of these techniques have the drawback of only being able to produce structures on planar substrates, such as those usually employed in cell culture. As few applications in tissue engineering call for two-dimensional (2D) scaffolds, the use of 3D scaffolds is necessary to impose functionality on cells that require structural cues during cell culture. Approaches to the production of 3D structures are usually focused on methods used in microelectronics applications, which tend to use non-biocompatible materials.[4] On the other hand, scaffolds produced from biocompatible or bioabsorbable materials tend to have limited control of surface topography.[5] At present there is no comparable microfabrication technique using a bioabsorbable material, and incorporating

[*] Dr. J. G. Fernandez, Dr. C. A. Mills, Prof. J. Samitier
Nanobioengineering Group
Institute for Bioengineering of Catalonia (IBEC)
c/ Josep Samitier 1–5, Barcelona 08028 (Spain)
Dr. J. G. Fernandez, Dr. C. A. Mills, Prof. J. Samitier
Networking Research Centre on Bioengineering
Biomaterials and Nanomedicine (CIBER-BBN)
Barcelona 08028 (Spain)
E-mail: jgfernandez@pcb.ub.es
Dr. J. G. Fernandez, Prof. J. Samitier
Department of Electronics, University of Barcelona
c/ Martí i Franquès 1, 08028 Barcelona (Spain)

DOI: 10.1002/smll.200800907

NANO MICRO small

microstructures, to produce 3D forms. We address this point by producing surfaces from a bioabsorbable polymer, chitosan, using a versatile production method.

In recent years, chitosan and its derivatives have been reported to have beneficial effects when applied to clinical or cell-culturing experiments,[6] as well as good mechanical and optical properties for industrial applications.[7] Although pure chitosan may not be a good candidate for some biological applications,[8] its capacity for chemical modification makes it adaptable to specific requirements, for example, drug delivery.[9] Here, we describe a method for the production of 3D chitosan structures containing microstructured surfaces, utilizing the rheological characteristics of chitosan in combination with its ability to be structured at the nanometer scale.[10]

To study the limits and versatility of our technique, it has been applied to the production of microstructured trenches and tubes with micrometer and millimeter internal dimensions, respectively, and by direct replication of the surface of a gelatin-based confectionary, emphasizing that the technique can be used to replicate delicate organic material with complex, rounded shapes. The resultant chitosan scaffolds have been demonstrated as possible grafts for tissue engineering, through the culture of endothelial cells on the surface of tubular scaffolds, and as secondary moulds for the production of structures in elastomeric polymers, such as poly(dimethyl siloxane) (PDMS).

2. Results and Discussion

The ability of chitosan to perform a reversible soluble–insoluble transition in response to environmental pH change has allowed us to develop a technique for building substrates with a predefined shape and highly controlled (sub)micrometer surface topography. The use of these surfaces in cell-culture experiments, for example, allows the cell culture properties to be controlled at the single-cell level via interactions with the structures on the surface, as well as conditioning cellular behavior as a group, by using a predefined form to mould the complete cell culture.

The tunable solubility of the polymer allows the production of 3D chitosan substrates, in two separate processes, with controlled topography at the (sub)micrometer scale. The chitosan molding technique (Figure 1) has been used to fabricate a number of 3D structures, all of which contain microstructures across their surfaces. Forced soft lithography (FSL)[11] is used to produce microstructures in planar chitosan films (Figure 1A) from which the macroscopic 3D form is produced (Figure 1B and C). Solid chitosan is a semicrystalline polymer with an orthorhombic unit cell containing two antiparallel chains. In the neutral state, the polymer is stabilized by hydrogen bonds formed in the polymer matrix by interstitial water molecules. Interaction with acetic acid, however, causes the structured chitosan films to have their NH_2 groups protonated (NH_3^+), introducing positive charge in the polymer matrix. The repulsive interchain electrostatic forces then permit further water molecules to enter the polymer matrix. Chitosan in this state behaves as an ionic polymer gel (IPG), absorbing liquid from the surrounding

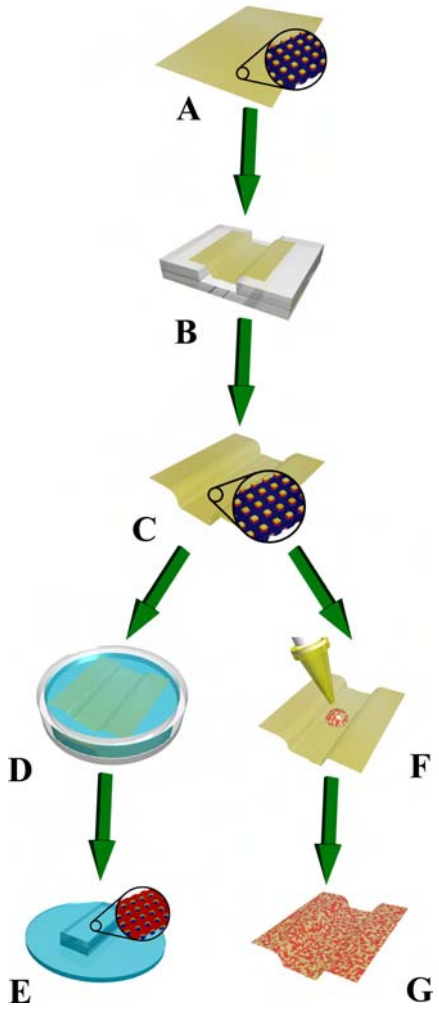

Figure 1. 3D structuring of microstructured chitosan. A) Chitosan is employed in an FSL process to produce planar, micro-, or nanostructured surfaces.[11] B) Controlled hydration of the film produces a (now flexible) film that can be deposited on a macroscopic mould to produce a 3D shape. C) After rigidification, the structured chitosan is separated from the mould. The chitosan structures can then be used for a number of applications, such as secondary replication in PDMS (D, E) or as substrates for cell culture (F, G).

medium in water-based solutions. This process is relatively slow, due to the diffusion of molecules through the gel. However, long immersion times cause dissolution of the polymer and will irreversibly damage the chitosan structures. At the extreme, the chitosan film will dissolve completely. The degree of hydration is inversely related to the stiffness of the (initially rigid) chitosan film and it is possible to explore the rigidity of the polymer between the solid and the liquid (gel-like) states by controlling the water absorption through the degree of protonation.

At low degrees of water absorption, the structured chitosan films are able to conform to the shape of a mould without losing the embossed structures. To achieve this level of hydration the chitosan is only briefly immersed in a low-concentration aqueous sodium hydroxide (NaOH) solution. The NaOH neutralizes some of the NH_3^+ sites, regenerating

the free amine (NH_2), and decreasing the solubility of the chitosan. However, the remaining NH_3^+ sites allow a partial hydration to occur and hence the polymer loses rigidity. The flexible chitosan film can then be used to cover a macroscopic mould, adopting the form of the support (Figure 1B). The chitosan–mould couple is then immersed in a higher concentration of NaOH to fully regenerate the amine groups and avoid later dissolution. Excess NaOH is rinsed off; the polymer is then dried and separated from the mould, leaving a freestanding microstructured replica (Figure 1C). The production of the 2D polymer films, used for the 3D structuring, is flexible enough such that small differences in chitosan quality are not likely to affect the production of the 3D shapes. Such surfaces can then be used for a number of applications, such as secondary moulds for elastomeric polymer replication (Figure 1D and E) or for direct use as biocompatible microstructured surfaces for cell–surface interaction studies (Figure 1F and G).

Examples of the flexibility of the method are presented in Figure 2. Figure 2A–D presents optical and scanning electron microscopy (SEM) images of a 1-mm-wide channel supported by a glass mould, which was employed for the production of the channel. The magnified images of the surface of the channel show the surface microstructures consisting of 1-μm-tall, 5×5-μm^2 square posts. Figure 2E–H gives an example of a microstructured tube produced from chitosan. Tubes with 1-mm diameter and of variable length, between 2 and 6 cm, have been produced. Figure 2I–L shows part of a chitosan replica of a gelatin-based confectionary containing 5-μm-diameter, 1-μm-deep hole microstructures across its surface.

Figure 2A presents an optical image of a 1-mm-wide channel supported by a glass mould. The chitosan channels, microstructured on the three walls that make up the channel, could be made using either glass or PDMS moulds without affecting the final results. The width of our channels could be defined between 2 mm and 150 μm, up to 1 cm in length. The length of the channel is only limited by the dimensions of the mould available for microstructuring in the FSL process (i.e., 1 cm in this case), and longer channels can be envisaged. However, the minimum width of the channel is limited by the mechanical properties of the chitosan film, namely, the ability of the chitosan to form into the corners of the mould.

Figure 2B–D shows the join between the floor and the wall at the edge of the channel in more detail. At small channel widths, the film does not completely adopt the shape of the sharp corners of the moulds, forming a rounded edge. To increase the capacity of the chitosan film to adopt the shape of the mould, several strategies are available. The choice of one method or the other depends on the final requirements of the chitosan structure. Decreasing the thickness of the chitosan film increases its capacity to form on the mould but gives rise to a mechanically weaker final structure. On the other hand, increased hydration of the chitosan will also increase the capacity to follow the shape of the mould but this may cause degradation of the microstructures on the chitosan surface (see explanation of Figure 5).

Figure 2E–H gives an example of a microstructured tube produced from chitosan. Two different approaches have been used to build the tube. The first method simply involves tightly wrapping the chitosan film around the glass mould. The second method produces a spiral-like junction (as shown in Figure 3). The drawback of the first technique is that the final chitosan structure is interrupted by the presence of the seam, between the two ends of the chitosan, which runs the entire length of the tube and can act as a source of weakness. Nevertheless, this technique is suitable for applications in which the microstructures are fabricated on the interior wall, and where the external

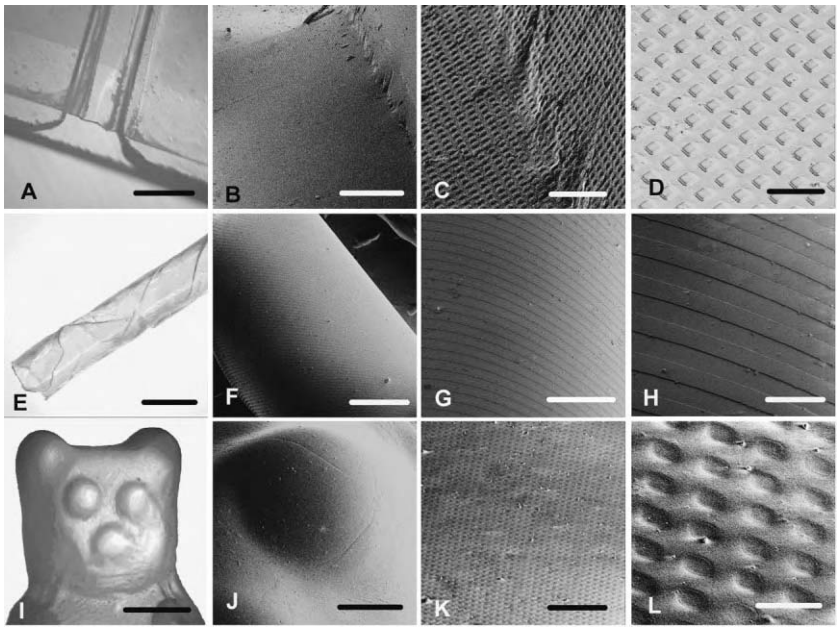

Figure 2. Versatility of the 3D chitosan structuring method. A) Optical microscopy image of a 1-mm-wide chitosan trench structured with square posts, 25 μm^2 and 1 μm tall, positioned on the glass mould used for fabrication (scale bar = 1.3 mm). B, C) SEM images of the structured area at the join between the floor and the wall of the trench (scale bars = 375 and 65 μm, respectively). D) Magnified area of the floor of the trench showing the microstructures in detail (scale bar = 30 μm). E) Optical microscopy image of a 1-mm-diameter spiral chitosan tube with microstructured channels, 1 μm deep, 10 μm wide, and with a 20-μm period, patterned on its surface (scale bar = 1.5 mm). F–H) SEM images of increasing magnification of the outer surface of the tube showing the structured channels, perpendicular to the longitudinal axis of the tube, in greater detail (scale bars = 400, 180, and 40 μm, respectively). Equally, the structures can be positioned on the inner surface of the tube by forming the reverse face of the chitosan around the mould. I) Optical microscopy image of the upper portion of a chitosan replica of a 2-cm-long bear-shaped gelatin-based confectionary with microstructured spherical holes on the surface (scale bar = 4 mm). J–L) SEM images of increasing magnification of the right eye area showing in greater detail the 5-μm diameter, 1-μm-deep microstructures in the chitosan surface (scale bars = 1000, 100, and 20 μm, respectively).

NANO MICRO small

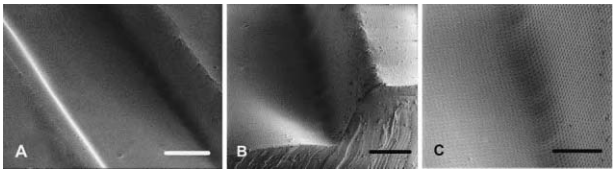

Figure 3. Rectangular PDMS channel with microstructured walls. A) SEM image of the 300-μm-wide channel structured with 1-μm-diameter holes (scale bar = 150 μm). B) Sectioning the channel reveals the channel shape and the thick PDMS walls (scale bar = 100 μm). C) Magnified SEM image of the wall and floor at the edge of the channel on which the microtopography can be seen (scale bar = 50 μm).

junction minimally affects processes occurring inside the tube. The second approach produces tubes with an improved strength and flexibility but introduces complexity in the fabrication because of the need to control (or eliminate) the overlap of the seam between each turn. Tubes with a diameter down to 400 μm have been produced via this technique by using glass capillaries, or needles, as the mould. However, it is assumed that the tube diameter in this case is only limited by the mould dimensions and smaller diameter tubes may be possible. The microstructures can be positioned either facing the capillary or facing away, giving rise to a tube with structures on its inner or outer surface, respectively, without damage to the structures.

To produce the 3-cm-long, 1-mm-diameter chitosan tube presented in Figure 2, we have employed a chitosan film 2-mm wide and 5-cm long, structured with 10-μm-wide channels. The chitosan was wrapped around a glass capillary in a partially hydrated state (immersed in NaOH solution, 2% v/v), forming a spiral with a 300-μm overlap on each turn. Once the chitosan is wrapped around the capillary, both are immersed in concentrated NaOH, then rinsed in distilled water and dried at room temperature. After drying, the support is easily removed because no chemical bonds are formed between the polymer and the glass, resulting in a freestanding chitosan tube. To the best of our knowledge, this is the first time that tubes with structured inner surfaces have been produced at these dimensions.

It is important to note that all the processes involving the production of the microstructured 3D scaffolds are completed at room temperature, allowing us to use delicate (organic) moulds. To show the versatility of the fabrication technique and to emphasize the ability to use organic moulds, we have utilized a bear-shaped gelatin-based confectionery (Figure 2I–L). In this case, the mould is based on edible gelatin, which is typically composed of up to 90% protein (18 different kinds of amino acids). The melting point of such gelatin-based confectioneries is within the range of human body temperature.[12]

In order to cast the chitosan film over this mould, the chitosan must contain a high concentration of protonated amine groups, requiring a slightly modified replication method. To reach such a state the chitosan film is immersed directly in distilled water for ≈0.5 s. During the immersion, the chitosan absorbs water, swells, and loses its rigidity. Care must be taken not to immerse the chitosan for too long, which may cause irreversible damage to the surface microstructures. Again, in the extreme state of protonation, complete dissolution of the chitosan film can occur. A thick film of structured chitosan (≈170 μm thick) is used for ease of handling and to avoid the possibility of tearing the polymer. The confectionary is then covered with the chitosan in its swelled state and immersed in ethanol. The (now molded) chitosan is finally separated from the gelatinous mould, immersed in a high-concentration NaOH solution (4% w/v) to regenerate the amine groups, and rinsed with water. In contrast to the previous examples, the mould–chitosan couple can not be immersed directly in NaOH because the confectionary tends to dissolve and stick to the chitosan film. Therefore, the two need to be separated before neutralization: the ethanol immersion provides sufficient rigidity to the chitosan to allow careful separation from the mould. Figure 2J–L presents magnified images of the right eye of the replica. The sphere has been faithfully replicated in the microstructured chitosan film and is shown to be completely covered in microstructures. Here, we replicate the mould in a way that allows us to remove the mould after replication. This leaves us with a 3D structure, microstructured on its entirety, with one face of the mould "open" to allow the mould to be removed.

Further replication is possible using PDMS, an elastomeric polymer with high chemical resistance and good mechanical properties, which makes it useful for a variety of applications including the production of microfluidic apparatus. A PDMS channel with 1-μm-diameter hole microstructures on all its walls, and replicated from a microstructured chitosan mould, is presented in Figure 3. A chitosan scaffold, containing 1-μm-tall post microstructures, was constructed in the same manner as for the microchannel presented in Figure 2A–D. However, this time, the microstructures were positioned facing the glass mould. The chitosan scaffold is placed upside down in a Petri dish and covered with liquid PDMS (Figure 1D), which, after curing and separation, produces a PDMS microchannel containing 1-μm-diameter holes (Figure 1E). Channels with widths from 150 μm to 1 mm, and a length of 2 cm, have been fabricated. Again, the selection of the topography, negative (i.e., holes) or positive (i.e., posts), is dependent on the application. We have produced topographical structures with areas from 1 to 100 μm^2.

The formation of 3D structures has been always a challenge in microfabrication but, in tissue engineering in particular, the production of tubelike scaffolds is fundamental because of the abundance of biological structures with this form. One particularly important example of an application is the production of artificial blood vessels. The fabrication of structured microtubes for microelectronic applications has been reported previously.[13] However, while the preceding techniques have produced a similar surface topography to that presented here, the materials used were not biocompatible and, up to now, no technique has been described that is suitable for the production of microstructured tubes using a bioabsorbable polymer, which can have applications in tissue engineering. The diameters of the tubes produced with our method are in the range where conventional synthetic grafts used for vein reconstruction fail. Conventional stents show excellent results when employed in large-diameter arteries (where arterial pressure is low) but have a high rate of failure

in arteries of less than 6 mm in diameter.[14] The corrugated structure imparted in our tubes enhances structural stability.

Arterial walls are composed of three cell layers (the intima, media, and adventia), with the intima being in contact with the lumen.[15] The arterial tissue has unique physical properties derived from the complex organization of proteins and cells. The intima is built of a single layer of endothelial cells and is considered to have a biological, rather than mechanical, role in the artery. It is responsible for providing a non-thrombogenic surface in contact with the blood and acts to regulate nutrient and water transport across the artery wall. A major stumbling block in the use of artificial artery walls is the poor mechanical strength of the artificial tube which, in most cases, is attributed to the orientation of the cells after their seeding on the scaffold.[16] Figure 4 shows optical microscopy images of human umbilical vein endothelial cells (HUVEC) after four days of culture on the surface of a chitosan tube structured with 1-μm-deep, 17-μm-wide channels running perpendicular to the tube length. The surface structures produce a passive conditioning of the direction of cell growth (i.e., the cells orient perpendicular to the longitudinal axis of the tube). In most cases, the nucleus of the cell (arrowed) tends to rest at the bottom of the channels, but, in all the cells, the cell membrane follows the direction imposed by the channels.

The capacity of the structures to control cell alignment depends on their height; the cell becomes insensitive to small structures but, on the other hand, excessively large structures will interfere with the natural connectivity of the tissue. Figure 4B shows that, in this case, the structures are tall enough to encourage cell alignment but low enough to allow interconnection of the cellular matrix over the channel walls. Consequently, over time, this allows a high degree of interconnection to occur and, eventually, the cells reach confluence (Figure 4D). The structures influence the alignment of the cells, at least at short culture times. However, the intercellular forces of subsequent layers of cells overcome the structural cues. In the case of cells growing on non-structured areas of the chitosan tube (Figure 4C), the cells are randomly aligned and no preferred growing direction is observed.

A chitosan film produced by the FSL process has most of its amino groups protonated, making it water soluble. In water, the structured chitosan film tends to dissolve, by the dissolution of the polymer chains into aqueous medium, causing a consequent degradation of the surface structures. To avoid this process it is necessary to neutralize the amine ($-NH_3^+$) groups in the chitosan by immersion in a basic solution, consequently improving the polymer interchain association.[17] The more basic the solution is, the faster the neutralization.

In a basic aqueous solution, two opposing processes are involved in the degradation of the topography. The dissolution of the chitosan polymer chains in the medium degrades the surface structures, while the neutralization of the amino groups enforces the structures by making the chitosan polymer chains increasingly insoluble. To measure the degradation of the structures during the molding process, we have measured the average height of seven structured samples before and after being immersed for 1 s in different aqueous NaOH solutions (Figure 5). Post immersion, the chitosan is neutralized in high-concentration NaOH (4% w/v), rinsed with distilled water, and dried before measuring. The samples have a 1-cm^2 area structured with 1-μm-tall, 5-μm-diameter circular posts. The average heights of the posts are measured by randomly choosing four points on the sample and studying a 124×94-μm^2 area (120 posts in each measurement) using white-light interferometry. The measurement is repeated after

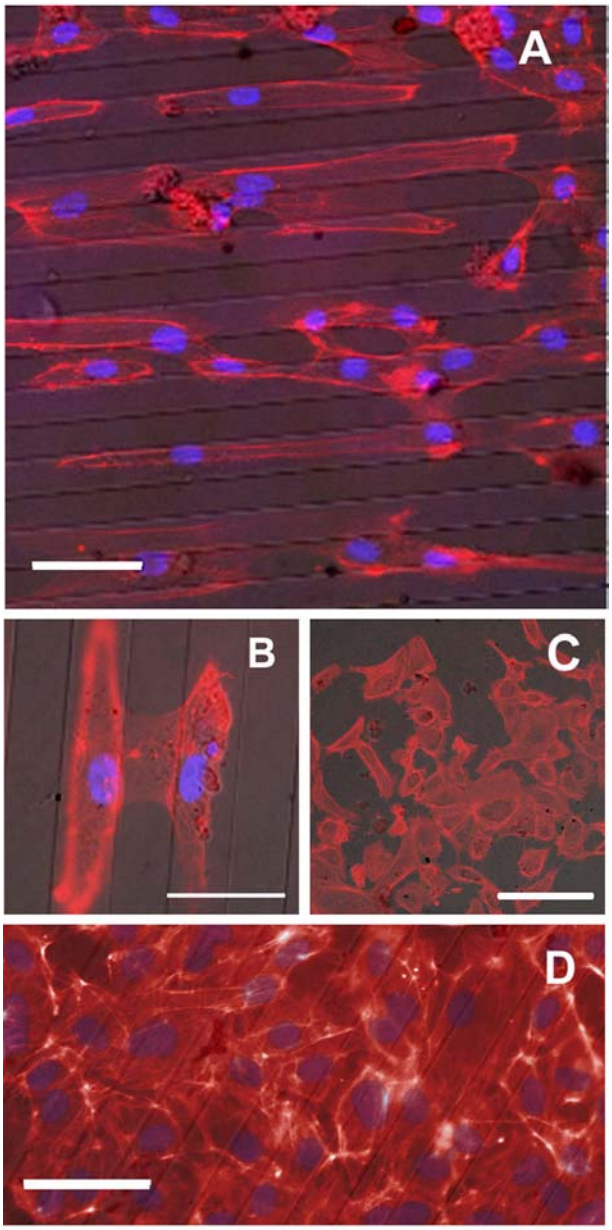

Figure 4. A) Fluorescent microscopy images of HUVEC cells cultured on the inner surface of a 1-mm-diameter chitosan tube structured with 17-μm-wide, 1-μm-deep channels positioned perpendicular to the long axis of the tube (scale bar = 45 μm). The cells can be seen to align to the direction of the channels. B) HUVEC cells positioned in separate channels extending their electrocellular matrix (ECM) over the adjoining 1-μm-tall wall to contact their neighbor (scale bar = 30 μm). Cell nuclei are indicated with arrows. C) HUVEC cells cultured on the non-structured areas of the tube display random alignment (scale bar = 120 μm). D) Confluent cells on the structured support after four days culture (scale bar = 50 μm).

NANO MICRO small

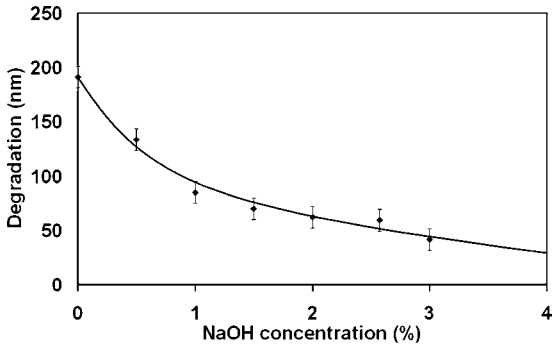

Figure 5. Graph showing the degradation of 1-μm-tall post structures on a planar chitosan surface when neutralized using increasingly concentrated aqueous NaOH solutions.

completing the hydration process and both results are compared to obtain the average decrease in height of the posts.

Treating the chitosan film with a 2% w/v (or greater) solution of NaOH (Figure 5) reduces the height degradation of the posts to less than 4% in 1-μm-tall structures and permits enough water absorption to produce all of the scaffolds presented here, except for when using the confectionary mould. As we suggested in the case of the microchannel, the concentration of NaOH used depends on the mould shape and the thickness of the chitosan film. Here, all of the fabricated samples are freestanding, requiring relatively thick chitosan films (≈170 μm thick) to allow them to be handled directly. For samples where the loss of several nanometers of material is too great, a very thin chitosan film must be used (possibly requiring a support, which is also flexible), which is able to mould the desired shape at high NaOH concentrations.

3. Conclusion

The soft-lithography technique presented here addresses the problem of replicating curved surfaces (shapes) in a bioabsorbable polymer/hydrogel with high replication fidelity, and introduces the possibility of both microscale and nanoscale topography control. The antigenic capacities and bioabsorbability of chitosan have already been used to produce templates for synthesis of neodermal tissue.[18] The addition of a determinate topography to the template, using our technique, will allow controlled cell growth, which may partially overcome the lack of functionality of the cells (absence of pores, etc.) in existing skin replacements.

Chitosan has also been tested as an intraocular drug-delivery system.[19] Due to its properties, such as optical clarity, mechanical stability, sufficient optical correction, gas permeability, wettability, and immunological compatibility, it has also been employed in contact lenses by spin coating on other polymers.[20] Again, our method, for the production of freestanding chitosan structures, could eliminate the need for a supporting material. The ability to organize culturing cells on such a scaffold may be useful in treating retinal diseases, for example, where the organization of the cells making up this sensitive part of the eye is crucial.

Finally, chitosan is useful in the absorption of metals and surfactants and also attracts basic dyes. Consequently, it is already being deployed for water treatment.[21] By micro- and nanostructuring the surface, the active surface area of the material increases and, consequently, increases the contaminant capture efficiency. Such a system would have advantages for cleaning water-based and biological fluids (e.g., blood), or for sensing systems.

4. Experimental Section

Materials: Medium-molecular-weight chitosan (75–85% deacetylated, 200–800 cps viscosity) derived from crab shell (Sigma-Aldrich Chemical Co., USA) was prepared as previously reported.[10] Silicon-based moulds containing the microstructures were produced using reactive ion etching (RIE).[22] The moulds consist of a silicon substrate coated with an oxide layer and then a thicker silicon nitride layer. The microstructures are defined in the nitride layer, which acts as an antiadhesive surface. Glass moulds for production of the 3D surfaces were prepared by arranging glass pieces of different thicknesses at set distances from each other and fixing them in place with the help of several presses. PDMS (Sylgard 184 Silicone Elastomer; Dow Corning, USA) was prepared using a standard method[23] and a pre-polymer/crosslinking agent ratio of 10:1, according to the manufacturer's recommendations.

Chitosan structuring: Microstructured chitosan surfaces were produced using an FSL technique.[11] Briefly, FSL consists of room-temperature molding of chitosan, from acetic acid solution, onto planar micro or nanostructured silicon or PDMS moulds. The process is aided by the application of external pressure, which forces air trapped in the mould cavities to dissolve into the bulk polymer solution. Solvent evaporation and then separation of the dried chitosan from the mould give rise to a micro/nanostructured film with the negative relief of the structures on the mould. Recently, similar results, imparting nano- and microstructures on planar chitosan substrates, have been obtained using a nano-imprinter and applying high temperature and pressure.[24]

To produce the 3D structures, the microstructured chitosan was immersed in a solution of sodium hydroxide (NaOH, 2% v/v) for ≈1 s. Partial gelation of the structured planar polymer surface occurs, which imparts flexibility into the chitosan and allows it to be molded to the surface relief of the moulds. The chitosan–mould couple is then immersed in a higher concentration of NaOH (4% v/v) for 10 min to fully regenerate the amine groups and avoid later dissolution. Excess NaOH is rinsed from the chitosan using distilled water (15 min). The polymer is then dried and separated from the mould, leaving a freestanding microstructured replica. The 3D structure fabrication procedure is presented in Figure 1.

Cell culture: Endothelial growth medium, supplement medium, and HUVEC from three different umbilical cords in the third passage were provided by Advancell (Spain). Chitosan tubes were immobilized on the bottom of a Petri dish and seeded at $\approx 1.5 \times 10^4$ cell cm^{-2}. As a bioreactor was not used for the cell culture, the tubes tend to be colonized only on their top surface. After 4 h, the tubes were moved to another Petri dish to eliminate cells growing on the Petri dish. At this point, the cellular growth medium (supplemented with 20% fetal calf serum (FCS)) was also

changed to ensure trypsin-EDTA (EDTA: ethylenediaminetetraacetic acid) solution is absent from the plating. Further changes of the medium were carried out, each for 36 h.

For the cell-alignment study, half of the tubes were immersed in glutaraldehyde solution (2.5%) for cell fixation and treated with hematoxylin and eosin dyes to color cell components for optical microscopy studies. The rest of the tubes are treated with paraformaldehyde solution (16%), opened and deposited on a microscope slide for confocal microscopy studies. Actin filaments and nuclei were dyed for fluorescence microscopy studies using the fluorescent dyes phalloidin-TRITC and Hoechst respectively (Sigma–Aldrich Chemical Co., USA).

Characterization: Simultaneous characterization of the micro- and macrostructure of the chitosan scaffolds was difficult to achieve due to the large 3D, microstructured surface topography. The structures were therefore characterized in multiple steps at increasing magnification in order to completely capture the available information, from the macroscopic shape to the surface micrometric characteristics. The scaffolds were first examined with an optical microscope to check the 3D shape and to confirm the existence of microstructures on the surface. Images with higher magnification were carried out using SEM (Strata DB35 dual beam FIB/SEM, FEI company, USA).

For quantitative analysis of the degradation of the microstructures on flat surfaces, replicas were examined using white-light interferometry (Wyko NT110, Vecco Metrology, USA) with a lateral resolution of 200 nm and nanometer vertical resolution. 500 micrometric structures were analyzed in four randomly chosen areas of each sample. Each measurement was repeated twice (before and after hydration of the chitosan film) to obtain the average decrease in height.

Acknowledgements

This paper and the work it concerns were generated in the context of the CellPROM project, funded by the European Community as contract No. NMP4-CT-2004-500039 and it reflects only the authors' views. Support for this work from the Spanish Ministry for Science and Education, through the provision of FPU (JGF) and Ramon y Cajal (CAM) grants, is also gratefully acknowledged. We thank A. Aguirre and M. Funes for their assistance in cell culturing, and M.-J. Lopez Bosque for help in the production of the SEM images. We also thank M. Rivas for providing the HUVEC cells and medium, and Dr. A. Errachid, Dr. C. Moormann, and Dr. T. Wahlbrink for supplying the microstructured moulds.

[1] a) M. J. Dalby, *Med. Eng. Phys.* **2005**, *27*, 730–742; b) M. J. Dalby, N. Gadegaard, R. Tare, A. Andar, M. O. Riehle, P. Herzyk, C. D. W. Wilkinson, R. O. C. Oreffo, *Nat. Mater.* **2007**, *6*, 997–1003.
[2] a) S. Y. Chou, P. R. Krauss, P. J. Renstrom, *Science* **1996**, *272*, 85–87; b) B. D. Gates, Q. Xu, M. Stewart, D. Ryan, C. G. Willson, G. M. Whitesides, *Chem. Rev.* **2005**, *105*, 1171–1196; c) S. Brittain, K. Paul, X.-M. Zhao, G. Whitesides, *Phys. World* **1998**, *11*, 31–36.
[3] a) A. Curtis, C. Wilkinson, *Biomaterials* **1997**, *18*, 1573–1583; b) C. D. W. Wilkinson, M. Riehle, M. Wood, J. Gallagher, A. S. G. Curtis, *Mater. Sci. Eng. C.* **2002**, *19*, 263–269.
[4] X.-G. Chen, C.-S. Liu, C.-G. Liu, X.-H. Meng, C. M. Lee, H.-J. Park, *Biochem. Eng. J.* **2006**, *27*, 269–274.
[5] S. J. Hollister, *Nat. Mater.* **2005**, *4*, 518–524.
[6] a) A. D. Martino, M. Sittinger, M. V. Risbud, *Biomaterials* **2005**, *26*, 5983–5990; b) S. Minami, M. Oh-oka, Y. Okamoto, K. Miyatake, A. Matsuhashi, Y. Shigemasa, Y. Fukumoto, *Carbohydr. Polym.* **1997**, *33*, 285–294; c) C. B. Machado, J. M. G. Ventura, A. F. Lemos, J. M. F. Ferreira, M. F. Leite, A. M. Goes, *Biomed. Mater.* **2007**, *2*, 124–131.
[7] a) P. R. Stoddart, P. J. Dadusch, T. M. Boyce, R. M. Erasmus, J. D. Comins, *Nanotechnology* **2006**, *17*, 680–686; b) J. Synowiecki, N. A. Al-Khateeb, *Crit. Rev. Food Sci. Nutrition* **2003**, *43*, 145–171.
[8] a) S. Minami, M. Oh-oka, Y. Okamoto, K. Miyatake, A. Matsuhashi, Y. Shigemasa, Y. Fukumoto, *Carbohydr. Polym.* **1996**, *29*, 241–246; b) M. I. Haque, A. C. Beekley, A. Gutowska, R. A. Reardon, P. Groo, S. P. Murray, C. Andersen, K. Azarow, *Curr. Surgery* **2001**, *58*, 77–80.
[9] a) K. Miyatake, Y. Okamoto, Y. Shigemasa, S. Tokura, S. Minami, *Carbohydr. Polym.* **2003**, *53*, 417–423; b) J. Murata, I. Saiki, T. Makabe, Y. Tsuta, S. Tokura, I. Azuma, *Cancer Res.* **1991**, *51*, 22–26.
[10] J. G. Fernandez, C. A. Mills, E. Martinez, M. J. Lopez-Bosque, X. Sisquella, A. Errachid, J. Samitier, *J. Biomed. Mater. Res. A* **2008**, *85*, 242–247.
[11] J. G. Fernandez, C. A. Mills, M. Pla-Roca, J. Samitier, *Adv. Mater.* **2008**, *19*, 3696–3701.
[12] GELITA Group Ltd. http://www.gelita.com.
[13] R. J. Jackman, S. T. Brittain, G. M. Whitesides, *J. Microelectromechanical Syst.* **1998**, *7*, 261–266.
[14] B. C. Isenberg, C. Williams, R. T. Tranquillo, *Circ. Res.* **2006**, *98*, 25–35.
[15] H. Gray, *Anatomy of the Human Body*, (Ed.: W. H. Lewis), Bartleby, Philadelphia **2000**.
[16] J. D. Kakisis, C. D. Liapis, C. Breuer, B. E. Sumpio, *J. Vascular Surgery* **2005**, *41*, 349–354.
[17] M. Yalpani, L. D. Hall, *Macromolecules* **1984**, *17*, 272–281.
[18] I. V. Yannas, J. F. Burke, D. P. Orgill, E. M. Skrabut, *Science* **1982**, *215*, 174–176.
[19] G. Di Colo, Y. Zambito, S. Burgalassi, I. Nardini, M. F. Saettone, *Int. J. Pharmaceutics* **2004**, *273*, 37–44.
[20] S. Xin-Yuan, T. Tian-Wei, *J. Bioactive Compatible Polym.* **2004**, *19*, 467–479.
[21] A. Gamage, F. Shahidi, *Food Chem.* **2007**, *104*, 989–996.
[22] C. A. Mills, E. Martinez, F. Bessueille, G. Villanueva, J. Bausells, J. Samitier, A. Errachid, *Microelectron. Eng.* **2005**, *78–79*, 695–700.
[23] Y. Xia, G. M. Whitesides, *Angew. Chem. Int. Ed.* **1998**, *37*, 550–575.
[24] I. Park, J. Cheng, A. P. Pisano, E.-S. Lee, J.-H. Jeong, *Appl. Phys. Let.* **2007**, *90*, 093902-3.

Received: June 26, 2008
Revised: September 2, 2008

